

# FIELD INVESTIGATION OF EVAPORATION FROM FRESHWATER TAILINGS

By Yoshimasa Fujiyasu,<sup>1</sup> Martin Fahey,<sup>2</sup> and Tim Newson<sup>3</sup>

**ABSTRACT:** Safe and economical storage of tailings is now a major consideration in the operation of many mining operations. Tailings in slurred form, particularly if they have a significant clay content, can take a very long time to consolidate under the action of self-weight consolidation alone. However, if the operation is located in an area of high potential evaporation, this can be used to accelerate the rate of tailings densification. This paper presents a study of the evaporation behavior of a clayey tailings slurry deposited into an evaporation pond in the southwest of Western Australia. Over a six-month period, the rate of evaporation from the tailings surface was monitored using the Bowen Ratio method and the microlysimeter method. This was compared with the evaporation from a Class A pan located nearby. The tailings underwent very significant cracking as drying proceeded, and it was found that these cracks had a significant influence on the overall rate of evaporation once the top surface of the deposit started to desaturate. A large strain consolidation model was used to model the behavior, and the algorithm used in this model to include the effects of evaporation is shown to provide a reasonable prediction of the observed evaporation behavior.

## INTRODUCTION

The mining industry is a major contributor to the economy of Australia in general, and Western Australia (WA) in particular. Many of the mining operations produce tailings in slurred form—the alumina, gold, nickel, mineral sands, and iron ore industries being good examples. After deposition in tailings storage areas, these tailings undergo sedimentation and consolidation to achieve a final strength and density.

In most parts of WA, the annual Class A pan evaporation rate varies from less than 2 m to over 4 m. These high evaporation rates can have a beneficial effect on the behavior of tailings, due to the increase in density and strength brought about by evaporation. Thus, an understanding of the evaporation behavior of tailings is important for the management of tailings disposal in WA and in any other areas with significant evaporation rates.

The amount of volumetric shrinkage during desiccation of a soil becomes significant with increase in the clay content of the soil. Soft clayey materials such as many tailings easily develop cracks due to this volumetric shrinkage. After initiation of cracks, evaporation occurs not only from the horizontal surface but also from the newly created vertical surfaces of the cracks. The evaporation from shrinkage cracks may be significant, and this contributes to water loss from the tailings.

The results of field and laboratory tests carried out by Adams and Hanks (1964), Adams et al. (1969), Selim and Kirkham (1970), Ritchie and Adams (1974), and Hatano et al. (1988) suggest that cracks may intensify water loss from the soil. In particular, after the top surface of the soil (tailings) becomes dry, evaporation from cracks may be a significant contribution to water loss from the soil.

Numerical modeling of tailings sedimentation and consoli-

dation is usually carried out using one-dimensional large strain consolidation models [such as the MinTaCo model described by Seneviratne et al. (1996)]. Since a simple one-dimensional moisture flow model does not account for evaporation from cracks, such a model may underestimate the evaporation rate from a tailings surface unless the effect of cracks is properly incorporated into the model. Abu-Hejleh and Znidarcic (1995) modified a one-dimensional model to take account of three-dimensional shrinkage, crack propagation, and evaporation from the cracks, though the method used to do so was approximate. In their model, they assumed that, once the shrinkage limit was reached at the top surface, no further evaporation from that surface occurred—in effect, the formation of a desiccated crust on the surface seals the surface, preventing further evaporation. This leads to the conclusion that very high potential evaporation rates can produce lower overall evaporation, because the surface sealing occurs much more quickly than if the potential rate had been lower. In a subsequent discussion, Newson and Fahey (1996) suggested that this assumption could be too conservative, since some evaporation still continues past this point even from the top surface. In addition, evaporation may continue well past this point from the vertical surfaces of the cracks; hence, the overall rate of evaporation can still be significant.

Thus, shrinkage cracks may have a significant effect on evaporation from a tailings surface, particularly at later stages of drying. However, to date, no theoretical or empirical model that correctly quantifies evaporation from cracks has been developed. This was one of the main aims of the work described in this paper.

The work was carried out on freshwater tailings, which is an important qualification, because much of the tailings produced by the gold industry in WA contain highly saline water. As shown elsewhere (Fahey and Fujiyasu 1994; Newson and Fahey 1998), such high levels of salinity have a severe effect on the evaporation behavior.

The observation of the behavior of freshwater tailings was carried out at “slimes” ponds at the Yoganup North Mine, a mineral sands mine located some 200 km south of Perth. The first stage of separation of the mineral sands from the rest of the soil involves washing out the clay and other fines; these “slimes” are dewatered by evaporation in these ponds prior to being replaced in the mine void. The study focused in particular on the effect of shrinkage cracks on evaporation. During the observation period, the tailings, which had a very high clay content, developed significant shrinkage cracks. Evaporation rates from (1) the entire surface; (2) the intact horizontal sur-

<sup>1</sup>Geotech. Engr., Kiso-Jiban Singapore Pte Ltd., 60 Kallang Pudding Rd. #02-00, Tan Jin Chwee Industrial Build., Singapore 349320; formerly, PhD Student, The Univ. of Western Australia, Nedlands, WA 6907, Australia.

<sup>2</sup>Assoc. Prof., Dept. of Civ. Engrg., The Univ. of Western Australia, Nedlands, WA 6907, Australia.

<sup>3</sup>Lect., Dept. of Civ. Engrs., Univ. of Dundee, Dundee, DD1 4HN, UK; formerly, Res. Fellow, The Univ. of Western Australia, Nedlands, WA 6907, Australia.

Note. Discussion open until November 1, 2000. To extend the closing date one month, a written request must be filed with the ASCE Manager of Journals. The manuscript for this paper was submitted for review and possible publication on April 23, 1999. This paper is part of the *Journal of Geotechnical and Geoenvironmental Engineering*, Vol. 126, No. 6, June, 2000. ©ASCE, ISSN 1090-0241/00/0006-0556-0567/\$8.00 + \$.50 per page. Paper No. 20736.

face; and (3) the vertical surface of cracks were measured throughout the test period.

A Class A evaporation pan was set up adjacent to the test site, and the evaporation rates measured with this pan were compared with the evaporation rates from the tailings surfaces. The evaporation pan used is identical to the U.S. Weather Bureau's Class A pan, which consists of a cylindrical galvanized steel pan, 1.22 m in diameter and 0.25 m deep, fitted with a bird guard. Readings were taken at 9 am each working day.

Based on the test results, two semiempirical methods of estimating the evaporation rates from cracked freshwater tailings surfaces are proposed.

## SITE DESCRIPTION

### Topography

The site is at an elevation between 35 and 50 m AHD. The site map (Fig. 1) shows the locations and scale of tailings ponds in the active mine area. East of the mine site, the land rises gently; to the west, the topography slopes gradually toward the coast, which is approximately 16 km away. Most of the lowland areas have been cleared for agricultural development, and the uplands east of the mine site are generally uncleared and covered with natural eucalypt vegetation. This mine was operated by Westralian Sands Ltd. (now Iluka Pty. Ltd.) for the recovery of mineral sands.

### Climate

The mine site experiences a Mediterranean-type climate of cool wet winters and hot dry summers. The average annual rainfall for the period 1979–1990 was 818 mm, and the annual Class A pan evaporation (with bird guard) is about 1,200–1,400 mm (Luke et al. 1987). The annual average temperature is 16.2°C. Temperature ranges from a mean minimum of 11.9°C in winter to a mean maximum of 21.2°C in summer.

A rain gauge and Class A evaporation pan (with bird guard) were installed at the site at the location shown in Fig. 1. The monthly evaporation and precipitation data measured over a 12-month period from March 1995 through February 1996 at

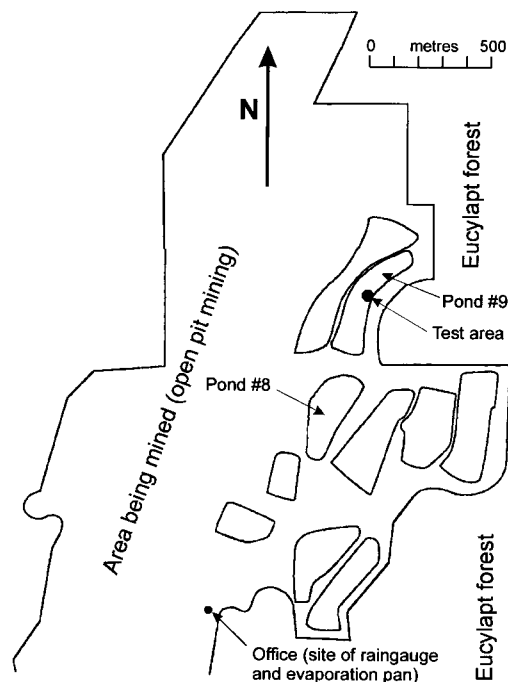


FIG. 1. Plan of Mine Area, Showing Location of Test Site in Pond #9, Yoganup North Mine

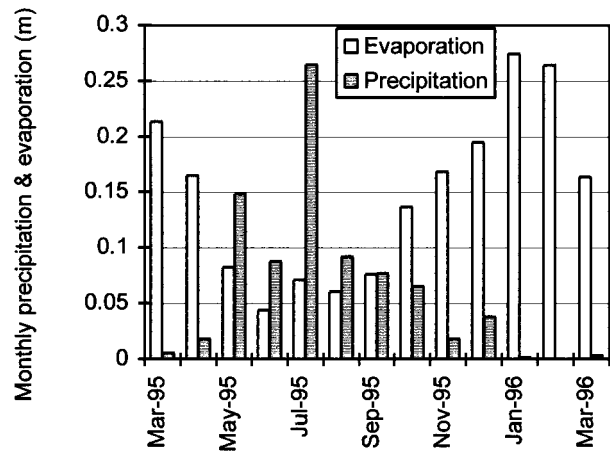


FIG. 2. Monthly Class A Pan Evaporation and Precipitation at Yoganup North Mine

the site are depicted in Fig. 2. In this period the total cumulative evaporation was 1,749 mm, with a total rainfall of 815 mm, giving a net evaporation of 934 mm. Rainfall exceeded evaporation in May, June, July, and August. Note that the rainfall is very close to the 1979–1990 average.

The day-time wind direction data recorded at Bunbury (20 km northwest of the mine site), which is the nearest available, indicated that summer and autumn winds are mostly from the southeast and southwest. Winds during spring are mostly from the southwest and northwest, while winter winds are mainly southwesterlies.

### Operation

The soil containing the heavy mineral sands are mined using dry mining (strip mining) techniques. In the hydraulic separation process that follows, the clayey fraction, which is predominantly kaolinite, is first separated from the sands by washing before the heavy minerals are separated from the lighter sands by gravity methods. The resulting dilute fine tailings or "slimes" are pumped via pipeline to large shallow evaporation ponds (approximately 2–3 m deep). At this stage, the water contents are between 2,000 and 3,000% (solids content between 3 and 5%). Sedimentation occurs rapidly, and the supernatant water passes over a recovery weir and is pumped back to the processing plant. The measured "sedimentation water content" of the tailings is about 350% (solids content of about 22%). When the ponds are full, they are left dormant for six months or more to allow the tailings to harden by consolidation and desiccation. They are then reexcavated and mixed back with the sand fraction for backfilling the open pit. These slimes ponds are the subject of the evaporation study described in this paper.

### Location of Field Test Sites

Observations of tailings drying behavior were carried out within two slime ponds, at four sites in Pond #8, and at one site in Pond #9. However, in this paper, only the results from Pond #9 are reported. This site is designated 9OZ (Pond #9 observation zone). These locations are shown in Fig. 1. The results from Pond #8 are presented by Fujiyasu (1997).

Pond #9 was built on a previously undisturbed area of bush. According to geological trends in the mine site, generally a sand layer lies at the surface, suggesting that the hydraulic conductivity of the base of Pond #9 is quite high. Tailings were pumped into Pond #9 from January 24, 1995, to April 19, 1995. At the end of filling, the depths of tailings was approximately 2–3 m.

## MATERIAL DESCRIPTION

Samples of the “as pumped” tailings were taken directly from the pipeline that transported the tailings to the drying ponds. The following soil tests were carried out using these tailings.

### Classification Tests

Analysis of a tailings water sample obtained from the thickener tank showed very low chemical concentration, with a total dissolved solids content of about 100 ppm. Thus, the tailings water can be taken to be effectively fresh water.

The properties of the tailings material are listed in Table 1. This indicates that the tailings material is a high plasticity clay. Analysis of the tailings using X-ray diffraction indicated 80% kaolinite, 10% quartz, and 10% goethite. The tailings are a deep red color when wet, due to the presence of iron oxides.

### One-Dimensional Consolidation Properties

Compressibility and hydraulic conductivity relationships of the test material were determined from centrifuge consolidation tests and conventional consolidation tests (using a Rowe cell). The results of these tests are presented as plots of void ratio versus effective stress in Fig. 3 and of hydraulic conductivity versus void ratio in Fig. 4. The curves fitted to the data are represented by the following equations:

$$e = 5.032 \times (\sigma'_v \text{ kPa})^{-0.254} \quad (1)$$

$$k = \left( \frac{e^{5.0}}{1 + e} \right) \times 10^{-5} \text{ (m/day)} \quad (2)$$

where  $k$  = hydraulic conductivity (m/day);  $e$  = void ratio; and  $\sigma'_v$  = vertical effective stress (kPa).

### Suction–Water Content Relationship

The suction–water content relationship for the tailings was determined by using the noncontact filter paper method (Faw-

TABLE 1. Soil Properties of Yoganup North Mine Tailings

Property (1)	Yoganup North Mine tailings (2)
Specific gravity ( $G_s$ )	2.70
Clay content (<2 $\mu\text{m}$ ) determined by hydrometer method	60%
Liquid limit, $w_L$	96
Plasticity index, $I_p$	61
Shrinkage limit	19

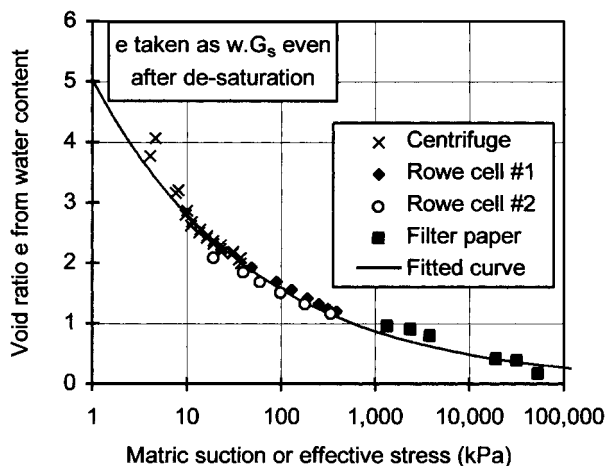


FIG. 3. Void Ratio versus Matric Suction or Vertical Effective Stress Relationships for Yoganup North Tailings

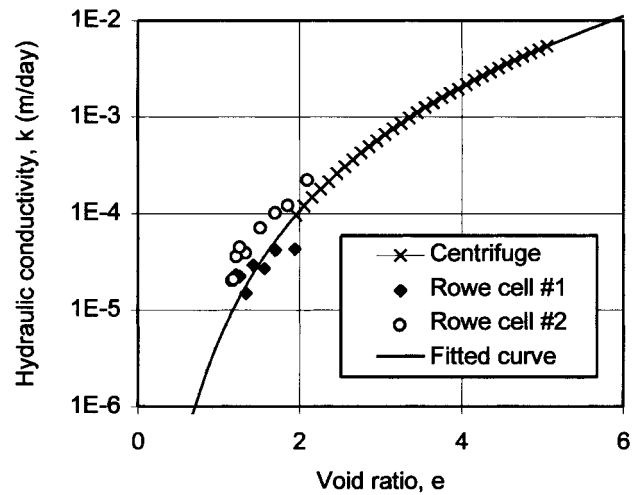


FIG. 4. Void Ratio versus Hydraulic Conductivity Relationships for Yoganup North Tailings

cett and Collis-George 1967; Chandler and Gutierrez 1986). Tailings obtained from various depths at Pond #9 were used for the tests. Since the chemical concentration in the tailings water was very low, the measured suction was regarded as the matric suction.

The results are included in Fig. 3 with the  $e - \sigma'_v$  relationship determined from the consolidation tests. (In effect, the void ratios shown relate to the ratio of the saturated void volume compared with the volume of solids, since the void ratio shown for the unsaturated samples was simply calculated as being  $w \cdot G_s$ , where  $w$  = water content.)

## EXPERIMENTAL PROCEDURE

### Observation of Tailings Drying Behavior

The layout of the field test site (90Z) in Pond #9 is shown in Fig. 5. The observations of crack growth were carried out in the  $5 \times 5$  m “crack observation zone” (COZ) shown in this figure. The depth of tailings at the beginning of May 1995 in the COZ was approximately 2 m. The dimensions (depth, width, and length) of all cracks developed in COZ were measured with a tape measure every few weeks until the tailings shrinkage ceased. Water content and vane shear strength profiles were frequently measured during the soil drying process (from May 1995 to March 1996) in the area surrounding the COZ, as shown in Fig. 5. Settlement of the tailings surface was measured relative to the tops of two steel rods that were driven into the sand below the base of the pond. All test activities were carried out carefully so as not to affect development of cracks.

Fig. 6 shows the test area at three different stages of drying. The COZ is outlined on these photographs.

### Direct Surface Evaporation Measurement

The “microlysimeter” method developed by Boast and Robertson (1982) was used to obtain direct measurements of surface evaporation from tailings. In essence, the method involves taking a 100 mm diameter by 100 mm long sample in a sample tube. The base of the tube is sealed, and the total weight is obtained. The tube is then put back into the ground such that the top of the sample in the tube is at the same level as the original ground surface. After 24 hours, the sample tube is retrieved, re-weighed, and the water loss obtained. The fact that the base of the sample tube is sealed has no effect on the evaporation rate from the surface over a 24 hour period (Boast and Robertson 1982), and so, provided that the surface sample

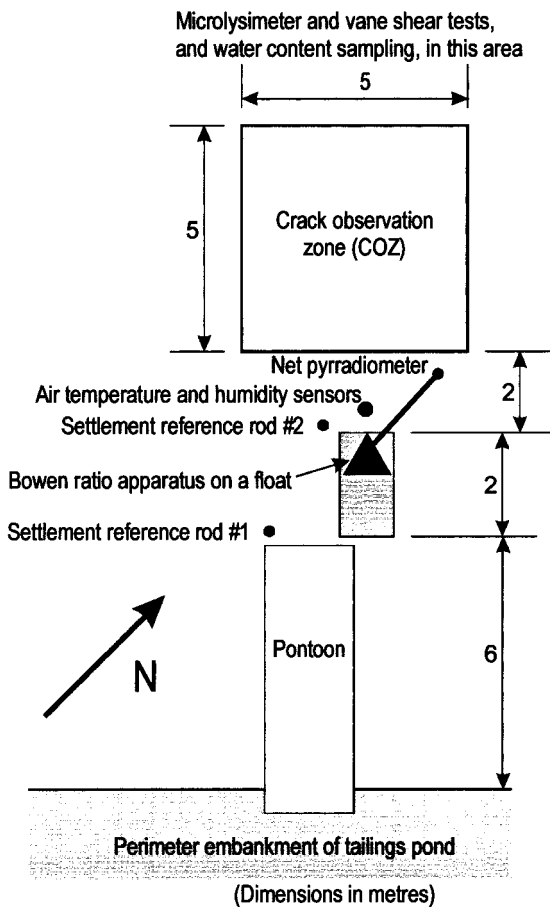


FIG. 5. Schematic Plan View of Arrangement at Test Site in Pond #9

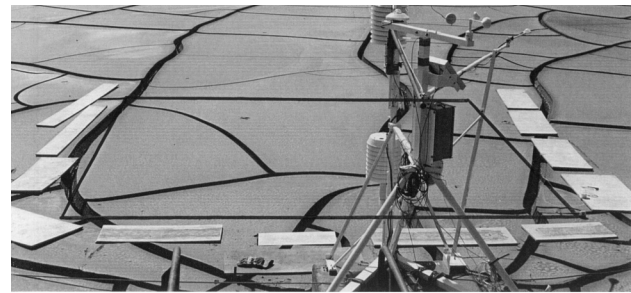
in the sample tube is the same as that of the surrounding undisturbed area, this 24-hour reading gives a good measure of the evaporation from that surface. In most of the tests, the tubes were made of PVC. These are preferable to metal tubes, because the high thermal conductivity of the latter could have an effect on the temperature in the sample and hence affect the evaporation rate.

A variation of the microlysimeter method was developed for determining the evaporation from the faces of cracks. The method used is illustrated in Fig. 7. A thin-walled aluminum alloy sampler, with the dimensions shown, is pushed down the face of the crack to the full depth of the sampler, and a sample is extracted. This sample is then subsectioned into a number of smaller samples, each of which is placed in an aluminum foil container. Each sample is weighed and replaced in its original position in the slot in the crack from which it was obtained. Re-weighing after 24 hours allows the loss due to evaporation to be obtained. Full details of the techniques used are given in Fujiyasu (1997).

Using these methods, evaporation from the top surface and from the vertical faces of shrinkage cracks was measured. In most of the cases, an identical cylindrical lysimeter filled with freshwater (water lysimeter) was used to monitor evaporation demand at the site where soil lysimeter tests were carried out.

### Indirect Surface Evaporation Measurement

The microlysimeter technique is an accurate, low-cost method of measuring the evaporation flux from a point on a bare soil surface. However, the technique does not allow continuous monitoring of evaporation flux when the test location is remote and the monitoring period is long. Moreover, the



(a)



(b)



(c)

FIG. 6. Crack Development in COZ at Three Different Dates: (a) 25 October 1995; (b) 16 November 1995; (c) 12 December 1995

evaporation flux from a cracked surface can be highly non-uniform and is difficult to estimate using this method.

The Bowen ratio approach (Bowen 1926) is one of the flux estimation methods that can be used to complement the microlysimeter technique. The net radiation energy  $R_n$  ( $\text{W/m}^2$ ) received at the ground surface is the algebraic sum of the incoming and outgoing short-wave radiation and the incoming and outgoing long-wave radiation. The energy balance equation for the ground surface may be written in the form

$$R_n = H + L_e E + G \quad (3)$$

where  $H$  = sensible upward (air) heat flux ( $\text{W/m}^2$ );  $L_e$  = latent heat of vaporization ( $\text{J/kg}$ );  $E$  = evaporation rate ( $\text{kg/m}^2 \cdot \text{s}$ ); and  $G$  = soil heat flux ( $\text{W/m}^2$ ), which is the heat flowing either downwards (+) into the ground, or upwards (-) towards the surface (the latter occurring at night). This equation states that the difference between all energy fluxes towards the ground surface and those away from it is equal to the heat used in evaporation. Thus, if the energy fluxes can be measured, the steady-state rate of evaporation can be determined. This is the basis of the Bowen ratio method of determining evaporation rate. This method partitions the available energy ( $R_n - G$ ) into sensible heat flux ( $H$ ) and latent heat ( $L_e E$ ), and expresses this as a ratio  $\beta$ , where

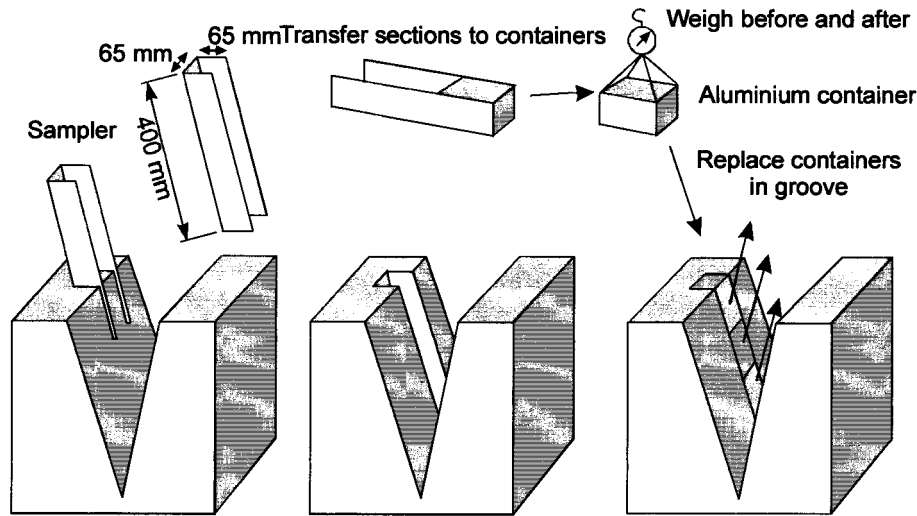


FIG. 7. Outline of Microlysimeter Technique Used to Determine Evaporation from Cracks

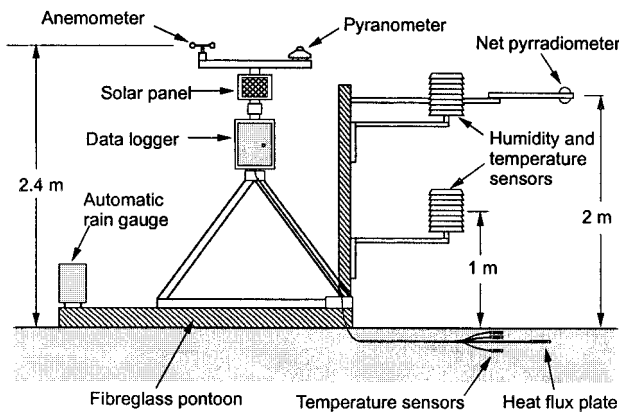


FIG. 8. Schematic View of Bowen Ratio Weather Station

$$\beta = \frac{H}{L_e E} = \frac{\rho c_{pm} K_h \frac{dT_d}{dz}}{\rho L_e K_v \frac{dh_s}{dz}} = \frac{c_{pm}}{L_e} \left( \frac{dT_d}{dh_s} \right) = \gamma \frac{dT_d}{dh_s} \quad (4)$$

In this equation, the thermodynamic value of the psychrometric constant  $\gamma = c_{pm}/L_e$ , where  $c_{pm}$  = specific heat ( $J/kg \cdot ^\circ C$ ) of moist air (density  $\rho$ ) at constant pressure. The equation states that  $\beta$  can be derived from changes in dry bulb temperature  $T_d$  ( $^\circ C$ ) and in specific humidity  $h_s$  ( $kg/kg$ ) over the same height interval  $dz$ . The quantities  $K_h$  and  $K_v$  ( $m^2/s$ ) are the eddy transfer coefficients of heat and water vapor, respectively, and are assumed to be equal in this approach. Thus,  $\beta$  is determined by measuring the dry bulb temperature and humidity at two different heights above the surface. The available energy is measured by determining the net radiation ( $R_n$ ) and the soil heat flux ( $G$ ), and  $E$  is then determined as

$$E = \frac{R_n - G}{L_e(\beta + 1)} \quad (5)$$

The Bowen ratio approach requires the use of a so-called Bowen ratio weather station. The weather station used is shown in Fig. 6, and a schematic drawing is given in Fig. 8. The instrumentation includes a pyranometer and net radiometer to measure net radiation ( $R_n$ ), humidity and temperature sensors located at 1 m and 2 m above the soil surface to measure the sensible heat flux ( $H$ ), and temperature and heat flux sensors in the soil to measure downward (or upward) soil heat flux ( $G$ ). The weather station was mounted on a fiberglass float at the site.

Some errors caused by: (1) "edge effects" due to the location of the station; and (2) the effect of the error in soil heat estimation were possible. However, the calculated evaporation rates compared very well with the values obtained from the volume change rates in the tailings, as discussed later, and hence appear to be reasonable. More detailed discussions on these effects can be found in Fujiyasu (1997).

## RESULTS AND DISCUSSION

### Overall Evaporation Behavior

Filling of tailings into Pond #9 was completed on March 19, 1995, and the depth of tailings measured on May 9, 1995, at 90Z was approximately 1,900 mm. Water content profiles through the tailings were determined at intervals by pushing a thin-walled sampler into the tailings and extracting core samples, which were subsampled to provide water content values. The drying of the tailings with time is illustrated by the plots of water content versus depth below the surface for various dates shown in Fig. 9, and by the plot of the water content of the upper 5 mm of the tailings surface versus time in Fig. 10. The shrinkage limit (19) for the tailings is indicated by the dashed line in each figure. This shows that prior to mid-January 1996, all of the profile probably remained fully saturated, and even when desaturation occurred at the surface, drying continued at all depths.

Fig. 11 shows a comparison of measured surface settlement and cumulative evaporation from a Class A pan, with condi-

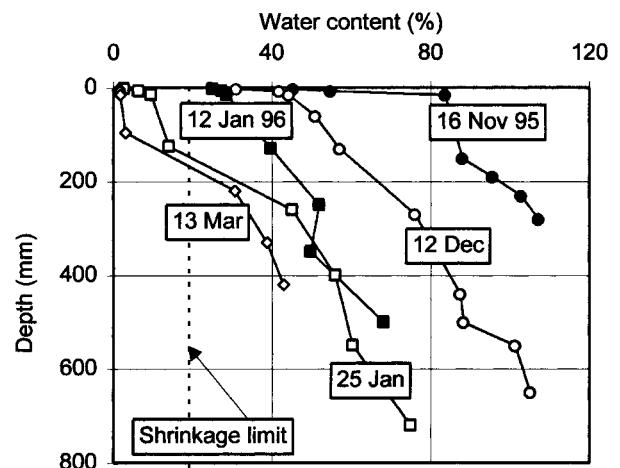


FIG. 9. Water Content Profiles at Different Dates in Pond #9

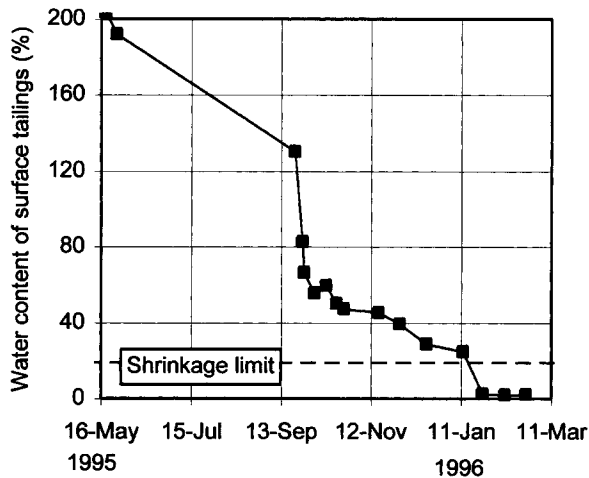


FIG. 10. Change in Surface Water Content with Time

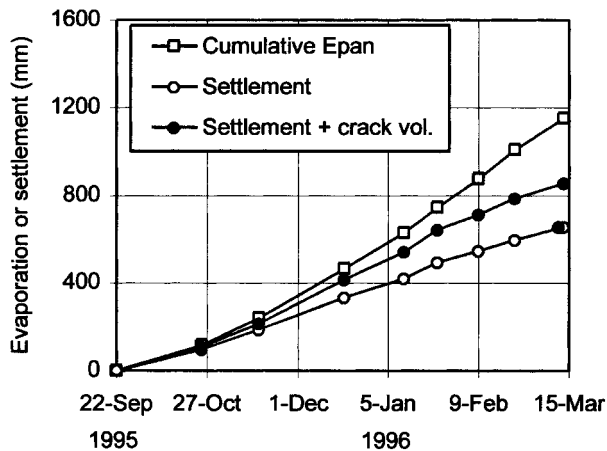
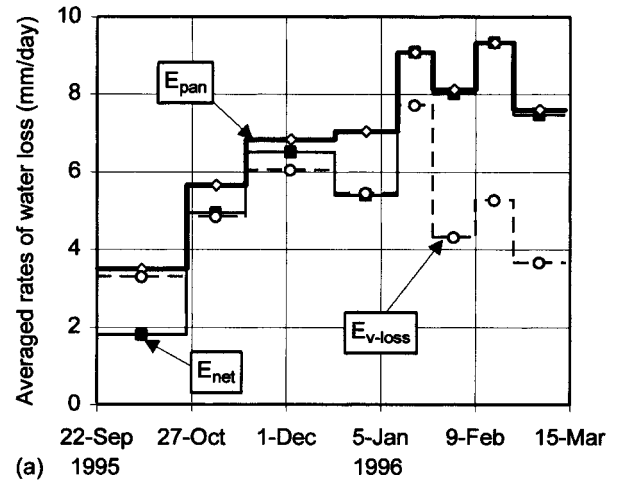


FIG. 11. Comparison of Surface Settlement and Cumulative Pan Evaporation

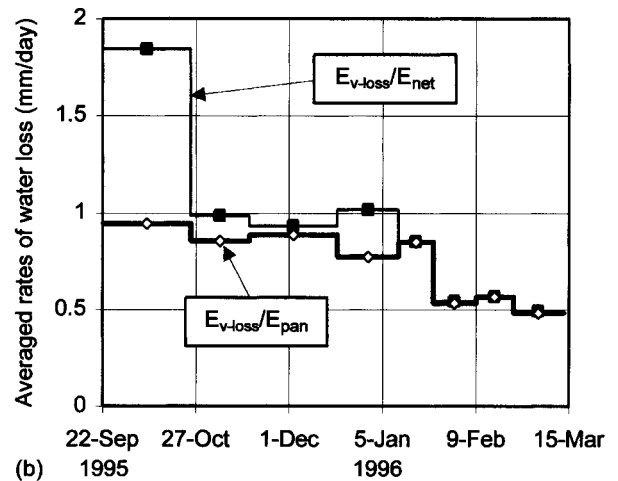
tions on September 22, 1995, being taken as the datum. Cracking only started to occur at about this date. Prior to this date, the total water loss deduced from the measured settlement is slightly greater than the cumulative pan evaporation. This is due to seepage through the base of the pond. However, from this date onwards, very little base seepage would have occurred (numerical modeling, discussed later, confirmed that this was the case); hence, the volume loss from the tailings is considered to be almost equal to the water loss due to evaporation during the period September 22, 1995, to March 4, 1996, in the following discussion.

In Fig. 11, the volume loss calculated from surface settlement is shown to lag behind the cumulative pan evaporation from early November 1995 onwards, even though desaturation of the surface did not start until early January 1996. However, when the volume of cracks is taken into account, much better agreement with the cumulative evaporation is obtained, as shown by the plot of total volume loss in this figure. The volume loss per unit area of tailings after initiation of cracks (at the end of September 1995) was calculated for the COZ as the sum of surface settlement and crack volume per unit area. In these calculations, the cross-sectional shape of a crack was assumed to be a triangle (becoming a trapezium after the crack reached the base of the pond), and the volume was then simply the cross-sectional area times the measured length of the crack.

Before the start of desaturation of the soil in early January 1996, the total volume lost by the tailings should be equal to the water loss from tailings. Even after desaturation started,



(a) Averaged rates of water loss (mm/day)



(b) Averaged rates of water loss (mm/day)

FIG. 12. Evaporation Rates Obtained from Class A Pan and Volume Loss Measurements

the water loss from the unsaturated zone would have been very small; hence, the volume loss would still be a reasonable estimation of the total water loss from the tailings.

It may therefore be concluded that the estimate of water loss based on the volume loss of the tailings (settlement plus volume of shrinkage cracks) is the best estimate of actual water loss from the tailings in the study period. In the subsequent discussion, this measurement of evaporation will be designated  $E_{v-loss}$ .

Using the data in Fig. 11, averaged rates (mm/day) of water loss ( $E_{v-loss}$ ) from the tailings after September 22, 1995, were calculated and plotted with averaged Class A pan rates in Fig. 12(a). The averages were obtained over periods indicated by the "steps" in the plots in this figure. Fig. 12(b) shows the average  $E_{v-loss}$  rates in the same periods normalized by both the Class A pan gross rate ( $E_{pan}$ ) and the Class A pan rate less the rainfall in the period ( $E_{net}$ ). This shows that the relative rates of water loss  $E_{v-loss}/E_{pan}$  were above 0.8 for the four-month period from October 1995 to January 1996. Thus, the evaporation rate from the tailings was very close to the pan evaporation rate in a period when the evaporation rate was moderate and the water content of tailings surface was sufficiently high. In February and March 1996, the combination of low water content near the tailings surface (see Fig. 9) and high evaporation demand reduced relative evaporation rates to 0.5–0.6. Thus, it can be said that the overall evaporation rate from the tailings had dropped to about 50% of the potential rate by the end of the study period. In the following sections, it will be shown that this relatively high rate was maintained

to the end mainly because of the growth of cracks in the tailings surface.

### Evaporation from Intact Horizontal Surface and from Cracks

Microlysimeter tests were carried out on areas of the intact horizontal surface in the zone surrounding the COZ (see Fig. 5). Two microlysimeters (one containing tailings that had been carefully sampled from the tailings surface and the other containing fresh water) were simultaneously used to measure daily values of tailings and fresh water evaporation (i.e., evaporation demand). The result of the tests are summarized in Fig. 13. In this figure, the rates shown are for a particular 24 hour period (whereas the data in Fig. 12 are average rates over extended periods). The three sets of data shown in Fig. 13 are from the Class A pan ( $E_{pan}$ ), the microlysimeter filled with freshwater ( $E_{fw-lys}$ ) and the microlysimeter filled with tailings ( $E_{soil-lys}$ ). The evaporation from the intact horizontal surface of the tailings was similar to  $E_{pan}$  and  $E_{fw-lys}$  up to and including the data obtained on January 11, 1996. The later readings show a severe reduction in evaporation rate from the intact horizontal tailings surface.

Evaporation occurred not only from intact horizontal surfaces but also from crack openings. The cracks gradually developed during the six months of the test period. The development of cracks observed in the COZ is illustrated in Fig. 14. The "open circle" symbols show the decrease in intact horizontal surface area due to shrinkage and cracking of the surface. In this figure, the intact horizontal surface area in the COZ is normalized by the initial total surface area ( $25 \text{ m}^2$ ). The cracks appeared at the end of September 1995, and the surface tailings shrunk continuously until the normalized horizontal surface area dropped to about 0.6 by the middle of January 1996. The behavior is consistent with the water content data in Figs. 9 and 10, which show that the water content of the tailings surface dropped below the shrinkage limit (19%) at about the middle of January 1996. Note that the water content profiles were determined from samples taken from positions more than 150 mm away from the nearest crack. Fig. 6 shows the crack development in the COZ. The area surrounded by the solid line indicates the crack observation zone (COZ). These photographs were taken on September 25, 1995, November 16, 1995, and December 12, 1995, respectively.

The "solid circle" symbols in Fig. 14 show the increase in total exposed surface area in the COZ, which includes the vertical surfaces of cracks and the intact horizontal surface area. In this plot, the total exposed surface area is normalized

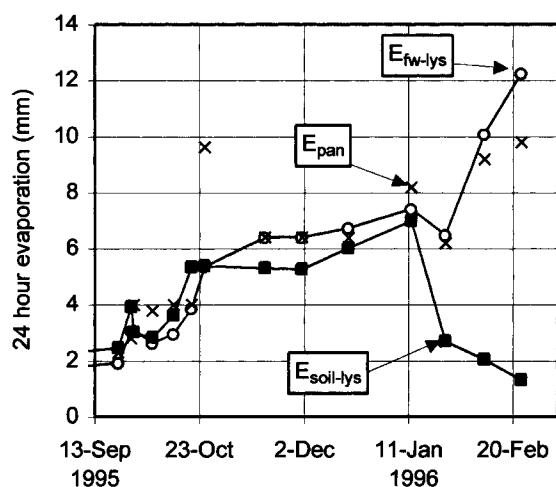


FIG. 13. Microlysimeter Test Results Compared to Pan Evaporation Data

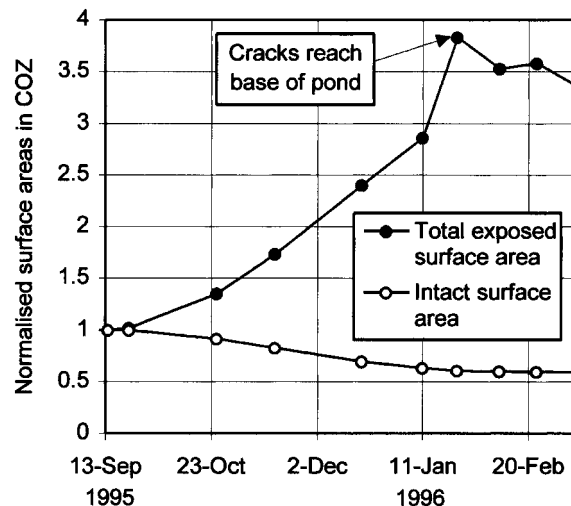


FIG. 14. Change in Intact Surface Area and Exposed Crack Surface Area Normalized by Initial Top Surface Area in COZ

by the initial exposed surface area ( $25 \text{ m}^2$ ). At the maximum, the total exposed surface area was 4 times larger than the initial value. After the cracks reached the base of the pond at the beginning of February 1996, no further increase in exposed surface area was possible and the value decreased from then on.

To determine evaporation from crack openings directly, the microlysimeter technique was applied to the vertical surfaces of the cracks, as explained previously (see Fig. 7). Fig. 15 shows some examples of evaporation profiles from vertical surfaces of cracks at various times, plotted against normalized depth in the crack (the depth normalized by the total depth of the crack). Dimensions (width and depth in mm) of each crack are also shown in these figures. Where water contents near the surface were high (on November 16, 1995, and December 18, 1995), evaporation rates were the highest at the surface and decreased monotonically with depth. However, as the top part of the cracks dried out, the highest evaporation rates occurred from points some distance below the surface (see data for January 14 and February 22, 1996).

Assuming the evaporation rates at the bottom of cracks (normalized depth = 1) were zero, evaporation rates from crack openings can be estimated by integrating the evaporation rates along the vertical crack surface. (The accuracy of these calculations is probably quite poor, so the following results should be viewed as being qualitative, rather than quantitative.) The values obtained were divided by the plan area of each crack opening and compared with the evaporation rates from the intact horizontal surface measured with vertically installed microlysimeters. Fig. 16(a) shows the measured data, compared with the  $E_{pan}$  values. It is emphasized that the actual evaporation rate per unit area of crack (vertical) surface is much less than shown here, since the actual surface area of each crack is much greater than the plan area of the crack opening.

The proportion of total evaporation coming from the cracks is shown in Fig. 16(b). This was obtained using the equation

$$\frac{E_{crack}}{E_{total}} = \frac{E_{crack} A_{crack}}{E_{crack} A_{crack} + E_{intact} A_{intact}} \quad (6)$$

where  $E_{crack}$  = evaporation rate from a unit plan area of crack opening as determined above;  $A_{crack}$  = horizontal surface area (plan area) of the crack opening;  $E_{intact}$  = evaporation rate from a unit area of intact horizontal surface; and  $A_{intact}$  = area of intact horizontal surface. This plot suggests that the percentage of evaporation from the crack opening continuously increased with the development of cracks, and at the end of February

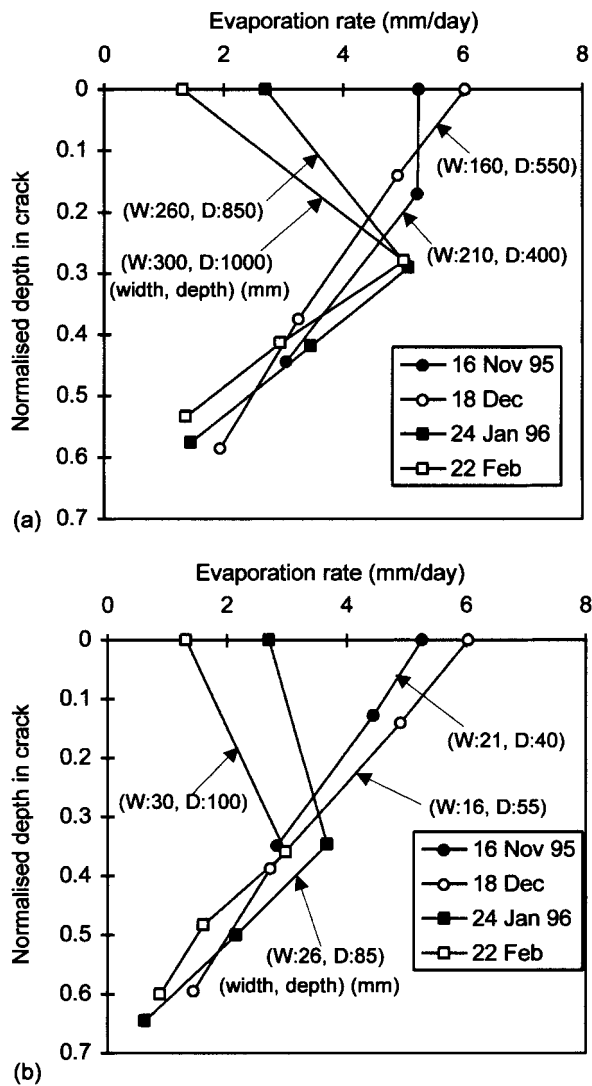


FIG. 15. Evaporation Rates from Vertical Surfaces of Cracks

1995, 80–90% of total evaporation was occurring from crack openings.

These results can be used to estimate the total evaporation rate per unit plan area (including cracks and intact surface). The result (labeled  $E_{total}$ ) is compared in Fig. 17 with the measurements made of total volume loss in the tailings ( $E_{v-loss}$ ) and the pan rate ( $E_{pan}$ ). This shows that the estimate based on measurement of evaporation from cracks is higher than  $E_{v-loss}$ , especially up to early January 1996. Since  $E_{v-loss}$  is regarded as the most accurate measurement of total evaporation loss, the estimate based on measurements from the cracks appears to be too high. This reinforces the point made earlier that the accuracy of this calculation is questionable, and the results should be regarded as being only qualitative. However, they do show that evaporation from cracks is important.

### Estimation of Evaporation Using Bowen Ratio Method

The Bowen ratio method of determining evaporation rate gives continuous readings with time. These readings are influenced by evaporation both from the intact surface and from the cracks. Fig. 18 shows a comparison of the daily rates determined by the Bowen ratio method,  $E_{Bowen}$ , and the averaged rates ( $E_{v-loss}$ ) calculated from the measured volume loss of the tailings in the COZ. As stated previously, the latter values ( $E_{v-loss}$ ) are taken to be the best estimate of overall evaporation

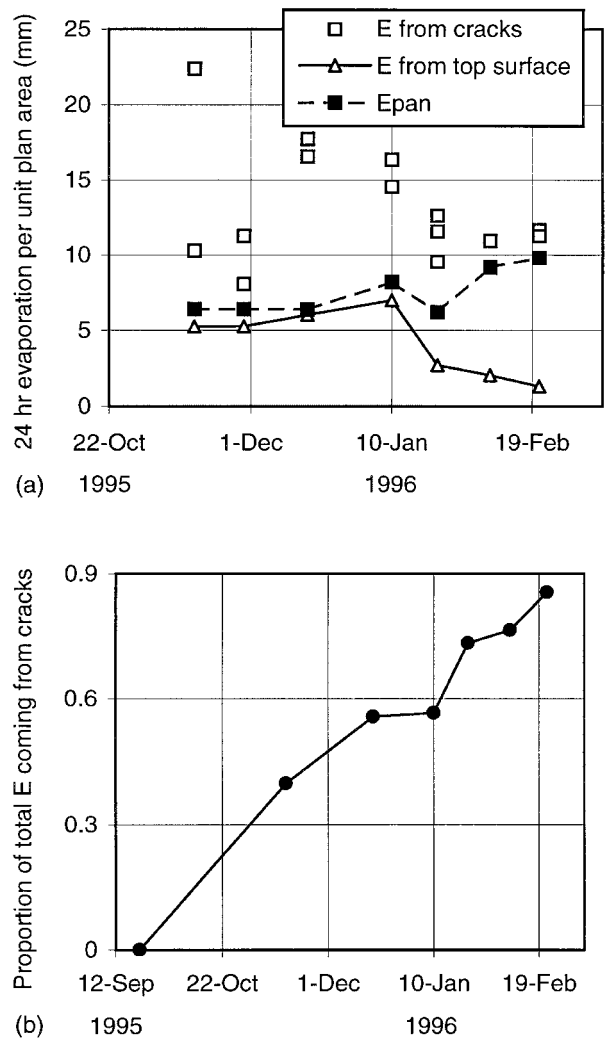


FIG. 16. Comparison of Evaporation Rates from Unit Plan Area of Crack Opening and Unit Area of Intact Surface: (a) Actual Rates; (b) Normalized by Intact Area

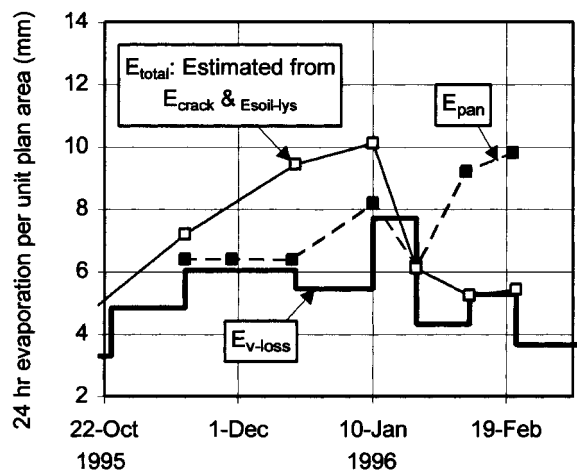


FIG. 17. Ratio of Evaporation from Crack Opening to Total Rate of Evaporation

loss. The Bowen rates are also averaged over the same periods as the  $E_{soil}$  values, and these are also shown plotted in this figure. This indicates that, while the daily Bowen ratio rates vary quite widely, the averaged measurements appear to be very similar to the rates deduced from the total volume loss. Thus, the tailings evaporation rates obtained from the Bowen ratio method supported the evaporation estimate obtained from



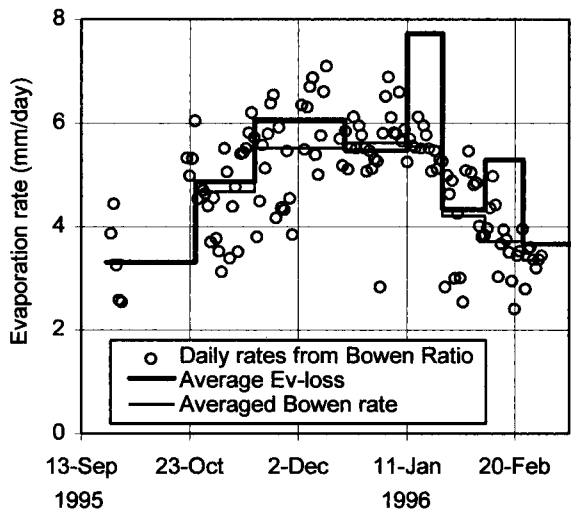


FIG. 18. Evaporation Rates from Bowen Ratio Method, Compared with Total Volume Loss

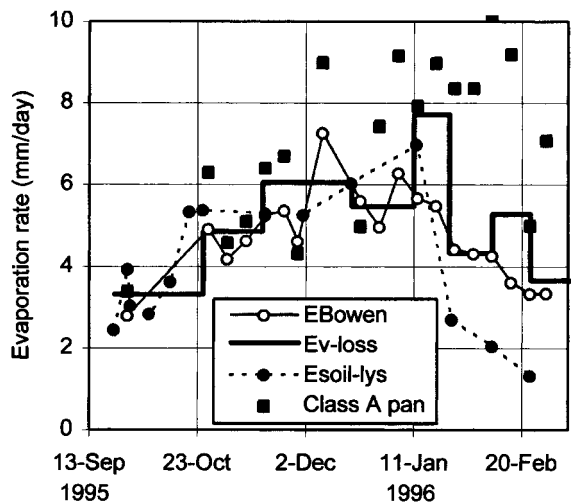


FIG. 19. Evaporation Rates from Bowen Ratio Method Compared with Evaporation from Pan, Volume Loss, and Measured from Intact Tailings Surface

volume change of the tailings in the COZ, and this confirms that the Bowen ratio method does not just measure the evaporation from the intact horizontal surface, but also includes the evaporation from the cracks.

Evaporation rates obtained by three different methods (i.e., volume loss measurement  $E_{v-loss}$ , Bowen ratio  $E_{Bowen}$ , and vertically installed microlysimeters  $E_{soil-lys}$ ) are plotted in Fig. 19, and Class A pan rates are also included for comparison. In this figure, the values  $E_{pan}$  and  $E_{Bowen}$  are weekly averaged values, while the  $E_{soil-lys}$  values are individual 24 hour readings. The volume loss measurements ( $E_{v-loss}$ ) are averaged over the intervals indicated by the “steps” in the plot. It can be seen from this figure that, whereas the rate of evaporation from the intact surface ( $E_{soil-lys}$ ) falls rapidly after January 11, 1996, the Bowen ratio measurements remain very close to the “true” rate (as determined by  $E_{v-loss}$ ), which reemphasizes that the Bowen ratio method takes account of the evaporation from the cracks and hence provides a good overall estimate of evaporation rate.

### SHEAR STRENGTH PROFILES

One of the effects of the combined consolidation and desiccation of the tailings is that the shear strength gradually increases. Vane shear tests were performed vertically down

through uncracked soil at locations 100–300 mm away from the nearest crack at various dates. The average depth of the adjacent cracks were also determined on the same dates. The measured vane shear strengths are shown plotted against depth in Fig. 20. On the curve for each profile of shear strength shown, a “solid circle” symbol on the curve indicates the depth of the crack on that date. The cracks reached the bottom of the tailings between February 9 and 23, 1996.

The maximum height ( $H$ ) of unsupported vertical face that can be sustained in a material with unit weight  $\gamma$  and undrained shear strength  $s_u$  is given by

$$H = \frac{2s_u}{\gamma} \quad (7)$$

Thus, a crack cannot form at some depth  $z$  unless the shear strength at that depth is greater than a critical strength

$$s_u(z)_{required} = 0.5\sigma_v(z) \quad (8)$$

where  $\sigma_v(z)$  = vertical total stress at depth  $z$ .

Knowing the vertical stress profile, the relationship between maximum possible crack depth and shear strength can be determined. Such a relationship, for December 12, 1995, is shown in Fig. 20 as the dashed line, labeled “max. possible crack depth.” The point where this line intersects the measured shear strength profile at that date is shown by a “solid square” symbol. This indicates that the maximum possible crack depth at this date was about 850 mm, compared with the measured depth of about 500 mm. However, it can be seen that the measured shear strength profile at this date shows low values at depths of around 500 mm, and the profile almost intersects the “max. possible crack depth” curve at this depth. Thus, it may be that this weaker layer prevented cracking developing to the maximum possible depth.

“Solid square” symbols are also shown on the shear strength profiles for October 13, 1995, and November 16, 1996, and indicate the maximum possible crack depths at these dates. In both cases, the agreement between the measured crack depth and the predicted maximum crack depth is quite good. Though not shown in Fig. 20, the maximum possible crack depth for the January 12, 1996, profile is just over 1,100 mm, which is somewhat deeper than the measured value.

It is clear from this very crude analysis that the depth of cracking is generally overpredicted by this approach. This is not surprising, since it does not take into account any of the other factors that contribute to crack depth determination (such as the work required to form a crack or the tensile strength of the soil resisting formation of a crack).

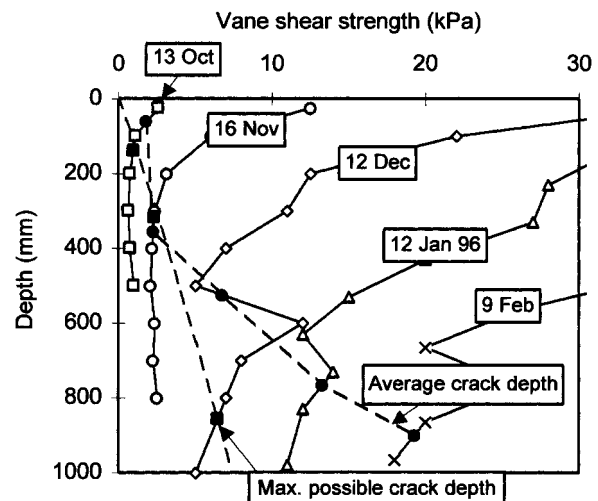


FIG. 20. Measured Vane Shear Strength versus Depth, and Average Crack Depth

## ANALYSIS OF TEST RESULTS

### Evaporation from Intact Horizontal Tailings Surface

A number of authors (e.g., Hillel 1971) have suggested that the evaporation behavior from granular porous media can be separated into two stages, the nonlimiting stage and the soil-limiting stage. In the nonlimiting stage, the evaporation rate is primarily controlled by the meteorological conditions, since there is always sufficient water available at the surface to meet the evaporative demand. The duration of this stage depends on the evaporation rate required by the atmospheric conditions and the ability of the soil profile to supply this rate. In the soil-limiting stage of drying, the water supply to the surface falls below that required by the atmospheric conditions, and evaporation from the soil is controlled by the moisture flow properties of the soil.

The measured evaporation behavior from intact horizontal surfaces in the test clearly showed these two stages of drying. The data presented previously in Fig. 13 show the evaporation rates obtained from freshwater lysimeters ( $E_{fw-lys}$ ) and lysimeters with tailings ( $E_{soil-lys}$ ) at the test location in Pond #9. The evaporation rate obtained from freshwater lysimeters can be taken to represent the potential evaporation rate (i.e., the evaporative demand). The combination of low evaporation demand and high water content at the tailings surface up to early January 1996 created a long period of nonlimiting drying. The soil-limiting stage of drying started at this time, when the surface water content fell below the shrinkage limit value (see Fig. 10). Since evaporative demand remained high from then on, the evaporation rates from intact horizontal surfaces decreased monotonically with time in accordance with the concept of soil-limited evaporation.

Thus, the evaporation behavior from intact horizontal surfaces of a tailings deposit can be clearly separated into two stages, the nonlimiting stage and the soil-limiting stage, in keeping with the generally accepted concept for drying of non-deformable porous media.

### Modeling Using MinTaCo Program

The MinTaCo (Mine Tailings Consolidation) program, developed originally by Toh (1992) and updated by Seneviratne et al. (1996), was used to model the evaporation behavior of the Yoganup North Mine tailings. Full details of this program are provided by Seneviratne et al. (1996) and will not be repeated here. This is a one-dimensional large-strain consolidation program that incorporates surface evaporation. While the water flow to the exposed surface is greater than the evaporative demand, evaporation has no effect (other than to remove water that could otherwise be decanted). However, once this flow rate falls below the evaporative demand, a suction is applied to the surface to produce a sufficiently high hydraulic gradient towards the surface to maintain the upward flow at the rate required to satisfy the evaporative demand. This suction is allowed to continue to increase until it reaches the air entry suction value for the soil (assumed to be equivalent to the shrinkage limit for tailings with a significant clay content). From then on, the suction is maintained at the shrinkage limit, and the evaporation rate falls rapidly below the potential rate. (In reality, the suction continues to increase, but the rapid reduction in hydraulic conductivity with the onset of desaturation has the same effect of rapidly reducing the evaporation rate.)

Since it deals with one-dimensional flow only, the MinTaCo program is not capable of modeling the effects of cracks. However, it is able to deal with evaporation from the intact horizontal surface. Therefore, it has been used to model the evaporation behavior at this site.

### Consolidation Parameters

The consolidation parameters represented by (1) and (2) were used in the modeling. The limiting value of suction was set at 8,000 kPa. This corresponds to the shrinkage limit of the tailings ( $e = 0.513$ ) and was calculated using (3).

### Boundary and Initial Conditions

For the top surface boundary condition, the potential evaporation rate ( $E_p$ ) for the tailings at Pond #9 was taken to be the measured average daily Class A pan evaporation rates ( $E_{pan}$ ) shown in Fig. 21 (average daily rates calculated from monthly totals in Fig. 2). At Pond #9, the tailings evaporation rates during the nonlimiting stage of drying were very similar to Class A pan evaporation rates, as shown previously in Fig. 13. Therefore,  $E_{pan}$  was considered to be an appropriate value for  $E_p$  for the modeling.

The soil-limiting stage of evaporation starts when the suction value at the tailings surface reaches the upper limit value, 8,000 kPa. Since the base material of Pond #9 was mainly sand, a fully permeable base boundary condition, with a fixed water table at the same level as the base, was assumed. Flow could occur downwards through this boundary, but upward flow was prevented (the model would have predicted upward flow from this boundary in the later stages of drying if this condition had not been applied).

Since the precise filling history of the pond was not available, the modeling had to be started from the "as filled" condition. The water content profile measured on September 22, 1995 (Fig. 22), was used as the basis for setting up the initial void ratio profile in the model, but some preliminary modeling work was required to determine an appropriate initial water content profile below the depths from which measurements had been made, particularly in view of the assumption of a drained base condition.

### Results

The water content profiles predicted by the MinTaCo program at various dates after September 22, 1995, are shown plotted against depth in Fig. 22. Even allowing for having adjusted the starting profile to agree with the measured profile on September 22, 1995, the agreement at subsequent dates is good. However, once desaturation occurs at the top surface, the measured water content at the surface falls rapidly towards

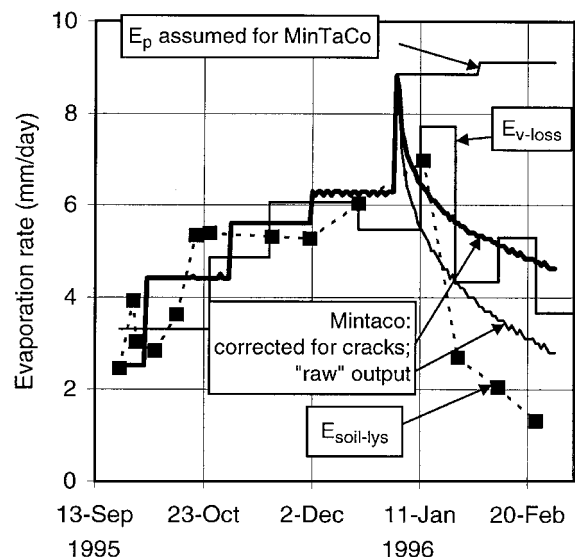


FIG. 21. Comparison of Measured Evaporation Rate with MinTaCo Output (Uncorrected, and Corrected for Crack Area)

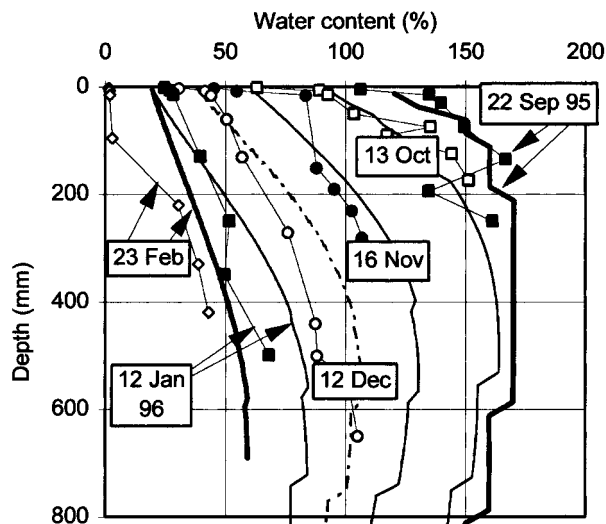


FIG. 22. Comparison of Water Content Profiles with MinTaCo Predictions

zero, whereas the algorithm used in the program does not allow the water content to fall below the point of air entry (the shrinkage limit of 19). Thus, whereas the measured water content profile on February 23, 1996, starts at about zero at the surface, the predicted profile starts at 19%. Note, however, that even though this limit of 19% is also indicated in the predicted profile for January 12, 1996, there is still some drying below the surface predicted between these two dates, and this is in agreement with the measured data.

The evaporation rates predicted by the MinTaCo program are compared with the measured values in Fig. 21. Two predicted rates are shown in this figure, one being the "raw" MinTaCo output, and the other the output corrected for the presence of cracks. This latter curve is discussed later. The measured data in this figure are the rates obtained from microlysimeters installed in the intact horizontal surface ( $E_{\text{soil-lys}}$ ) and the rates deduced from the measured volume loss ( $E_{\text{v-loss}}$ ). The latter are averaged over the periods between volume measurements, whereas the former are 24 hour averages for individual days.

During the nonlimiting stage of evaporation (prior to early January 1996), the predicted rate is identical to the input potential evaporation rate ( $E_p$ ), since this is the imposed boundary condition in the modeling. It has been shown previously that the measured rate is reasonably consistent with the potential rate in this period; hence, imposing this as a boundary condition is a reasonable approach to use. After the shrinkage limit is reached, the predicted evaporation rate starts to fall off rapidly, as expected. In this period, the predicted rate is higher than the rates measured from the intact surface ( $E_{\text{soil-lys}}$ ), but lower than the rates obtained from the measurement of volume loss ( $E_{\text{v-loss}}$ ). The latter includes the effect of cracks, but the former does not. Thus, the algorithm used to model evaporation in the soil-limiting stage of evaporation appears to overpredict the evaporation rate from an intact surface and, in the absence of cracks, would therefore be conservative (in terms of predicting the drying rate). However, where cracking occurs, it might be unconservative. Nevertheless, the overall pattern predicted is reasonable.

#### Correction for Effects of Cracks

It has already been shown that, for the material at this site, the cracks that developed in the surface contributed significantly to water loss from the tailings. Thus, Fig. 17 showed that, even before the rate of evaporation from the intact horizontal surface began to fall below the potential evaporation

rate (in January 1996), the cracks were contributing over 50% to the total evaporation rate, and subsequently this increased to almost 90%.

The total evaporation rate from a tailings surface with shrinkage cracks may be described by the following equation:

$$E_{\text{total}} = E_{\text{intact}} \frac{A_{\text{intact}}}{A_{\text{total}}} + E_{\text{crack}} \frac{A_{\text{crack}}}{A_{\text{total}}} \quad (9)$$

where  $A_{\text{total}}$  = total surface area; the definitions of  $A_{\text{intact}}$  and  $A_{\text{crack}}$  are as given previously [see (6)]; and  $E_{\text{intact}}$  and  $E_{\text{crack}}$  = rates of evaporation from the intact horizontal surface and the plan area of the cracks, respectively. Note that  $A_{\text{crack}}$  refers to the plan area of the crack openings and not to the total exposed surface area in the cracks. The ratio  $A_{\text{intact}}/A_{\text{total}}$  at any time during the drying stage may be calculated using the surface void ratio at that time ( $e_t$ ) and the surface void ratio at crack initiation  $e_i$  ( $e_t < e_i$ ):

$$\frac{A_{\text{intact}}}{A_{\text{total}}} = \left( \frac{1 + e_t}{1 + e_i} \right)^{2/3} \quad (10)$$

The basis for this equation is that the void ratio change results from volumetric shrinkage, which at the surface is likely to be isotropic, and since

$$\frac{V_{\text{total}}}{V_{\text{intact}}} = \left( \frac{1 + e_t}{1 + e_i} \right) \quad (11)$$

then the ratio of areas is equal to the ratio of volumes to the power of 2/3.

For the Yoganup North Mine tailings, cracking commenced on about September 20, 1995, when the surface water content had dropped to about 56% (see Fig. 10), which is equivalent to  $e_i$  equal to 1.51. This value was used with (10) to give the ratio of intact to cracked areas as a function of the surface water content computed by MinTaCo.

In order to use (9), an estimate of  $E_{\text{crack}}$  is required, and this is not usually available. It has been shown that the rate of evaporation from the cracks (when expressed as total evaporation from the cracks per unit plan area of the cracks) can be considerably greater than the pan evaporation rate. Therefore, the pan evaporation rate could be taken to be a reasonable lower-bound estimate of  $E_{\text{crack}}$ .

Taking this approach, a correction has been applied to the MinTaCo prediction of evaporation rate, which effectively assumes that

$$E_{\text{total}} = E_{\text{intact}} \frac{A_{\text{intact}}}{A_{\text{total}}} + E_p \frac{A_{\text{crack}}}{A_{\text{total}}} \quad (12)$$

where  $E_{\text{intact}}$  = rate predicted by MinTaCo; and  $E_p$  = input potential rate. The resulting corrected curve is shown plotted with the uncorrected curve in Fig. 21. It can be seen from this figure that the correction has given an overall evaporation rate somewhat closer to the total rate measured for this site.

## CONCLUSIONS

The evaporation behavior of freshwater tailings was monitored by using the microlysimeter technique and the Bowen ratio method and by measuring the volume loss of the tailings for over practically a full drying cycle. During this drying cycle, the growth of cracks in the tailings was monitored, and measurements were made of the evaporation rate from the sides of cracks, in order to provide an estimate of the contribution of cracks to the overall evaporation rate. The findings of this work are summarized as follows:

1. The method used to determine the total volume loss in

- the observation area, consisting of careful monitoring of surface settlement and measurement of crack volume, appears to have provided the best estimate of total evaporation loss from the tailings; hence, this is taken as the benchmark value. Obtaining these types of measurements would not be practical in most situations.
- Due to the development of shrinkage cracks, the total exposed surface area of the tailings became as large as four times the original crack-free surface area. Evaporation from a unit plan area of crack opening was consistently larger than  $E_{\text{pan}}$  during the observation period and contributed significantly to water loss from the tailings, especially in the later stages of drying. It was estimated that more than about 80% of the total evaporation occurred from cracks after the horizontal surface of the tailings started to desaturate.
  - The microlysimeter readings obtained on the horizontal surface provide a very good point measurement of evaporation, but this method underpredicts the total evaporation once this surface starts to desaturate, because it does not take account of evaporation from cracks.
  - The Bowen ratio method appears to take some account of the evaporation from cracks and hence provides a better means of determining overall evaporation rate. The fact that it is continuous, and automatic, is also a major advantage of this method.
  - When the tailings surface was sufficiently wet, evaporation from the tailings surface occurred at a similar rate to Class A pan evaporation. Thus, Class A pan evaporation appeared to be a very good approximation of the potential evaporation rate for the tailings ponds at the Yoganup North Mine. Of course, the overall evaporation from a unit plan area of cracked tailings surface can be significantly greater than the pan rate, because of the large exposed area of the crack faces per unit plan area of crack opening.
  - A simple way of estimating the maximum crack depth was suggested. This method gives a first-order approximation of the actual crack depth, but generally tends to overestimate the crack depth.
  - The evaporation rates from intact horizontal surfaces of the freshwater tailings observed in the field showed two drying stages, the nonlimiting stage and the soil-limiting stage. These two stages of evaporation were modeled using the MinTaCo computer code. Though the algorithm used to model the behavior after the shrinkage limit is reached at the surface is not in accordance with what actually happens, the model produced the correct pattern of rapid reduction in evaporation rate from that point onwards. This was found to be close to, but somewhat greater than, the rates measured from the intact horizontal surface at this stage.
  - The MinTaCo model is a one-dimensional consolidation and evaporation model and hence cannot model the contribution of cracks to the overall evaporation rate. However, a simple (and crude) method of adjusting the MinTaCo output to allow for cracks was suggested, and the adjusted MinTaCo output agreed somewhat more closely with the measured total evaporation rate.

## ACKNOWLEDGMENTS

The work described in this paper was carried out while the first writer was a PhD student and the third writer was a postdoctoral research fellow in the Department of Civil Engineering at The University of Western Australia. The first writer was supported by an Overseas Postgraduate Research Studentship from the Commonwealth Government of Australia. The work was supported by grants from the Australian Research Council and the Minerals and Energy Research Institute of Western Australia (MERIWA). This support is gratefully acknowledged. The financial and logistical support provided for this part of the work by Westralian Sands Ltd. (now Iluka Pty. Ltd.), the owners of the Yoganup North Mine, is also gratefully acknowledged, with particular acknowledgment to Mr. Jamie Warnock, who carried out the daily pan evaporation measurements at the site.

## APPENDIX. REFERENCES

- Abu-Hejleh, A. N., and Znidarcic, D. (1995). "Desiccation theory for soft cohesive soils." *J. Geotech. Engrg.*, ASCE, 121(6), 493–502.
- Adams, J. E., and Hanks, R. J. (1964). "Evaporation from soil shrinkage cracks." *Soil Sci. Soc. Am. Proc.*, 28, 281–284.
- Adams, J. E., Ritchie, J. T., Burnett, E., and Fryrear, D. W. (1969). "Evaporation from a simulated soil shrinkage crack." *Soil Sci. Soc. Am. Proc.*, 33, 609–613.
- Boast, C. W., and Robertson, T. M. (1982). "A 'micro-lysimeter' method for determining evaporation from bare soil: description and laboratory evaluation." *Soil Sci. Soc. Am. J.*, 46, 689–696.
- Bowen, I. S. (1926). "The ratio of heat losses by conduction and by evaporation from any water surface." *Physical Rev.*, 27, 779–787.
- Chandler, R. J., and Gutierrez, C. I. (1986). "The filter-paper method of suction measurement." *Géotechnique*, London, 36(2), 265–268.
- Fahey, M., and Fujiyasu, Y. (1994). "The influence of evaporation on the consolidation behaviour of gold tailings." *Proc., 1st Int. Congress on Envir. Geotechnics*, BiTech Publishers, Vancouver, Canada, 481–486.
- Fawcett, R. G., and Collis-George, N. (1967). "A filter paper method for determining the moisture characteristics of soil." *Australian J. Experimental Agric. and Animal Husbandry*, 7, 162–167.
- Fujiyasu, Y. (1997). "Evaporation behaviour of tailings." PhD thesis, Dept. of Civ. Engrg., The University of Western Australia, Nedlands, Australia.
- Hatano, R., Nakamoto, H., Sakuma, T., and Okajima, H. (1988). "Evapotranspiration in cracked clay field soil." *Soil Sci. Plant Nutrition*, 34(4), 547–555.
- Hillel, D. (1971). *Soil and water: physical principles and processes*. Academic Press, New York.
- Luke, G. J., Burke, K. L., and O'Brien, T. M. (1987). "Evaporation data for Western Australia." *Tech. Rep. No. 65*, Div. of Resour. Mgmt., Western Australian Department of Agriculture, South Perth, Australia.
- Newson, T. A., and Fahey, M. (1998). "Saline tailings disposal and decommissioning." *Rep. on MERIWA Project M241, Rep. No. ACG: 1004-98*, Australian Ctr. for Geomech., The University of Western Australia, Nedlands, Australia.
- Newson, T. A., Fahey, M., and Fujiyasu, Y. (1996). "Discussion on 'Desiccation theory for soft cohesive soils,' by A. Naser Abu-Hejleh and Dobroslav Znidarcic." *J. Geotech. Engrg.*, ASCE, 122(11), 944–946.
- Ritchie, J. T., and Adams, J. E. (1974). "Field measurement of evaporation from soil shrinkage cracks." *Soil Sci. Soc. Am. Proc.*, 38, 131–134.
- Selim, H. M., and Kirkham, D. (1970). "Soil temperature and water content changes during drying as influenced by cracks: a laboratory experiment." *Soil Sci. Soc. Am. Proc.*, 34, 565–569.
- Seneviratne, N. H., Fahey, M., Newson, T. A., and Fujiyasu, Y. (1996). "Numerical modeling of consolidation and evaporation of slurried mine tailings." *Int. J. Numer. and Analytical Methods in Geomech.*, 20, 647–671.
- Toh, S. H. (1992). "Numerical and centrifuge modelling of mine tailings consolidation." PhD thesis, Dept. of Civ. Engrg., The University of Western Australia, Nedlands, Australia.